

Turbulent Relaxation to a Force-Free Field-Reversed State

Jill P. Dahlburg

U.S. Naval Research Laboratory, Washington, D.C. 20375

David Montgomery

Dartmouth College, Hanover, New Hampshire 03755

and

Gary D. Doolen and Leaf Turner

Los Alamos National Laboratory, University of California, Los Alamos, New Mexico 87545

(Received 4 February 1986)

The evolution of nonequilibrium initial conditions of an incompressible magnetohydrodynamic Z pinch is described by a three-dimensional, pseudospectral numerical code. Magnetohydrodynamic turbulence develops in the resistive, nonviscous magnetofluid, resulting in the selective decay of the energy relative to the magnetic helicity, at Lundquist numbers of only a few hundred. An interior force-free region grows with time and achieves spontaneous reversal of the toroidal magnetic field at the wall, without the necessity of an external electric field.

PACS numbers: 52.55.Ez, 47.65.+a, 52.65.+z

Theoretical or computational treatments of magnetohydrodynamic (MHD) pinches usually have been described in terms of the evolution of unstable normal modes of laminar equilibria. However, the formation of Z pinches can be violent, and there may be regimes in which laminar equilibrium conditions are never a good initial approximation.¹⁻³ The nonlinear evolution of the resulting magnetic and velocity fields is of interest. In explaining Z -pinch behavior, it has been conjectured⁴⁻⁶ that the resulting MHD turbulence leads to a "selective decay"⁷⁻¹⁰ of energy relative to magnetic helicity. This idea has received some numerical support in two dimensions,^{8,9} with axisymmetry,¹⁰ and in three dimensions^{11,12} (see the recent review by Hasegawa¹³). The physical bases of "selective decay" turbulent processes have been presented in Refs. 7-10 and 13.

The nature of selective decay becomes clear from the spectral representations of the two ideal invariants, energy and magnetic helicity. The former derives a higher fraction of its contributions from the larger wave numbers, where the dissipation occurs, and so is more affected by the decay of the short-spatial-scale expansion coefficients. The result is a decrease in ratio of the energy to magnetic helicity. At the lower limit of this ratio, a "force-free" state results.¹⁴ For high enough currents, and a given toroidal magnetic flux, this implies reversal of the toroidal component of the magnetic field near the outer wall,⁴⁻⁶ thought to be desirable for the achievement of quiescence and confinement.

We report nonlinear MHD turbulence computations of evolving Z pinches which achieve spontaneous self-reversal of the toroidal magnetic field at the wall. The computation does *not* contain (1) external electric

fields, (2) initial regions of diminished toroidal flux near the wall ("aided" reversal), or (3) finite compressibility. We use broad-band-noise initial conditions not close to an equilibrium and a Lundquist number S of a few hundred. There is no viscous stress. Related, but significantly different, computations have been reported by Sykes and Wesson¹¹; Aydemir and Barnes¹⁵; Schnack, Caramana, and Nebel¹⁶; Werley, Nebel, and Wurden¹⁷; and Horiuchi and Sato.¹⁸ The present calculation is closest to that of Aydemir and Barnes¹⁵ and Horiuchi and Sato.¹² Our novel features include (1) a demonstrable connection between field reversal and selective decay to a force-free state; (2) much lower values of S (a few hundred here, as contrasted with $\geq 5 \times 10^4$ in Ref. 15); and (3) broad-band-noise nonequilibrium initial conditions, giving about as much small-scale turbulence as the dissipation will permit. The turbulence, the relaxation, and the force-free state are all aspects of a single process.

We solve the one-fluid incompressible MHD equations in a region which is periodic in the z direction and is terminated by a smooth, square, rigid, perfectly conducting boundary in the x and y (poloidal) directions. In a standard set of dimensionless variables, the square poloidal boundary has edge length π and the periodicity length in z is 2π . The dimensionless induction equation is $\partial \mathbf{B} / \partial t = \nabla \times (\mathbf{v} \times [\mathbf{B} + \mathbf{B}_0]) + S^{-1} \nabla^2 \mathbf{B}$, where \mathbf{v} is the velocity field, the total magnetic field is $\mathbf{B}_{\text{tot}} = \mathbf{B}_0 + \mathbf{B}$, and S is the Lundquist number, or dimensionless conductivity. The magnetic field $\mathbf{B}_{\text{tot}} = B_0 \hat{\mathbf{e}}_z + \mathbf{B}$, where B_0 is a uniform constant. $\nabla \cdot \mathbf{v} = 0$ and $\nabla \cdot \mathbf{B} = 0$.

The numerics are a direct outgrowth of a 3D code^{19,20} recently used to solve the Strauss equations

of "reduced" MHD. A new and central feature of this code is that the boundary conditions are implemented by the Turner-Christiansen functions²¹ as a pseudo-spectral expansion basis rather than Fourier sine and cosine series. The variable part of the magnetic field is written as $\mathbf{B} = \nabla \times \mathbf{A}$, where

$$\begin{aligned} \mathbf{A}(x,y,z,t) &= \sum_{j,k,l} [a_{jkl} \chi_{jkl} + b_{jkl} \Xi_{jkl}], \\ \chi_{jkl} &= \nabla \times \phi_{jkl} \hat{\mathbf{e}}_z, \quad \Xi_{jkl} = \nabla \times (\nabla \times \psi_{jkl} \hat{\mathbf{e}}_z), \\ \phi_{jkl} &= (\cos jx)(\cos ky) \exp(ik_z z), \end{aligned}$$

and

$$\begin{aligned} \psi_{jkl} &= (\sin jx)(\sin ky) \exp(ik_z z); \\ \mathbf{B} &= \sum_{j,k,l} [a_{jkl} \mathbf{P}_{jkl} + b_{jkl} \mathbf{T}_{jkl}], \\ \mathbf{v} &= \sum_{j,k,l} [r_{jkl} \mathbf{P}_{jkl} + s_{jkl} \mathbf{T}_{jkl}], \end{aligned}$$

and

$$\mathbf{P}_{jkl} = \nabla \times \chi_{jkl}, \quad \mathbf{T}_{jkl} = \nabla \times \Xi_{jkl}.$$

The summations on the integer transverse-mode labels typically run from zero to 16 or 32, and for $l = k_z$, typically 16, 32, or 64. There are usually larger spatial derivatives in z ("n numbers") than there are in x and y ("m numbers") which develop dynamically. As a test of the code, we have set $S^{-1} = 0$ and run the code through various segments of field-reversal simulations. At a time of rapid change, while the code with resistivity lost 5.4% of the total energy in 0.6 Alfvén transit times, the code run in the ideal mode conserved total energy to $(4 \times 10^{-3})\%$.

Turbulent activation early in the run has been achieved by our picking the initial current $\mathbf{j} = j_z(x,y;0) \hat{\mathbf{e}}_z$ only, where $j_z = (\sin x)(\sin y) \{10 - 9 \times \exp(-3[x - (\pi/2)]^2 - 3[y - (\pi/2)]^2)\}$. We illustrate the results of about ten runs by describing in some detail a run with $S = 500$. Random noise with r_{jkl} and s_{jkl} of order 10^{-3} is loaded initially into those modes with j, k in the interval [4,8], and $\pm l$ in the range [1,12]. The hollow current profile (which does not stay hollow very long) is thought not to be unrealistic for pinches initiated by sudden wall electric fields, and has been found by trial and error to generate turbulence efficiently in a few Alfvén transit times of unit distance (a unit of time). The hollow current profile is one way, among others, of generating a large amount of small-scale MHD activity on Alfvénic time scales. The evolution is highly nonlinear, and is not simply relatable to any known instability on any known equilibrium.

Magnetic-field-line plots for B_x, B_y in an xy cut and B_x, B_z in an xz cut are shown in Figs. 1(a) and 1(b). Many modes are involved. Aximuthal Fourier analysis around the largest circle that will fit inside the computational square reveals that the largest contribution to the poloidal mode-number spectrum, for $m = 1, 2,$

..., 16, is $m = 1$. Several global integral quantities, volume averaged, are shown in Fig. 2.

Selective decay toward the relaxed minimum-energy state is illustrated by a 3D perspective plot of the alignment cosine, $\mathbf{j} \cdot \mathbf{B}_{\text{tot}}/jB_{\text{tot}}$, for times $t = 19.68$ and $t = 35.04$ in Fig. 3. The precipitous drop in energy-to-helicity ratio accompanies the formation of an interior region, nearly force-free, and a boundary layer of MHD activity which persists to the end of the run ($t = 35.04$). \mathbf{j} and \mathbf{B}_{tot} obey different boundary conditions at a perfect conductor,²¹ and cannot align themselves perfectly at a wall.¹⁰ So far, the relaxation to the force-free state has proceeded more dramatically than the relaxation to a minimum-energy state, as evinced by the greater constancy of the direction cosine, as compared with plots of $\lambda = \mathbf{j} \cdot \mathbf{B}_{\text{tot}}/B_{\text{tot}}$.² The further extent of relaxation to a force-free, minimum-energy state is being computed. Figure 4 shows an average $\langle B_{\text{tot}z} \rangle$ over the outer wall, with $S = 150, 500,$ and 1500 . If S is too low, the current decays to an extent that \mathbf{B} (whose curl \mathbf{j} is) cannot overcome \mathbf{B}_0 . If S is too large, too much small-scale turbulence develops for the code to resolve (e.g., at $S = 500$ and $16 \times 16 \times 64$ resolution; 15 h of Cray-2 time were required; doubling the resolution would have required 120 h).

Difficulties in resolving small scales at even modest S are nontrivial. In Fig. 5, magnetic-energy spectra and Ohmic-dissipation spectra are plotted in an uncon-

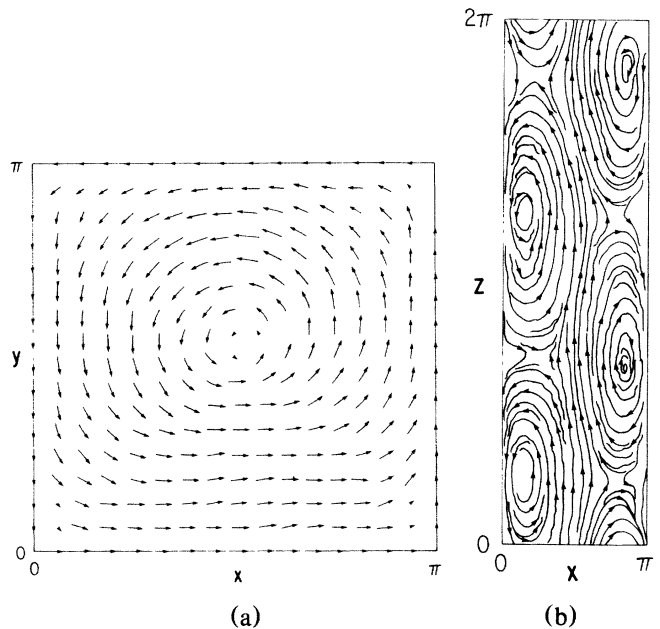


FIG. 1. (a) Magnetic field lines projected into the xy plane at $z = 0$, and (b) magnetic field lines of $\mathbf{B}_{\text{tot}} - \mathbf{B}$, projected into the xz plane at $y = \pi/2$ and time $t = 35.04$.

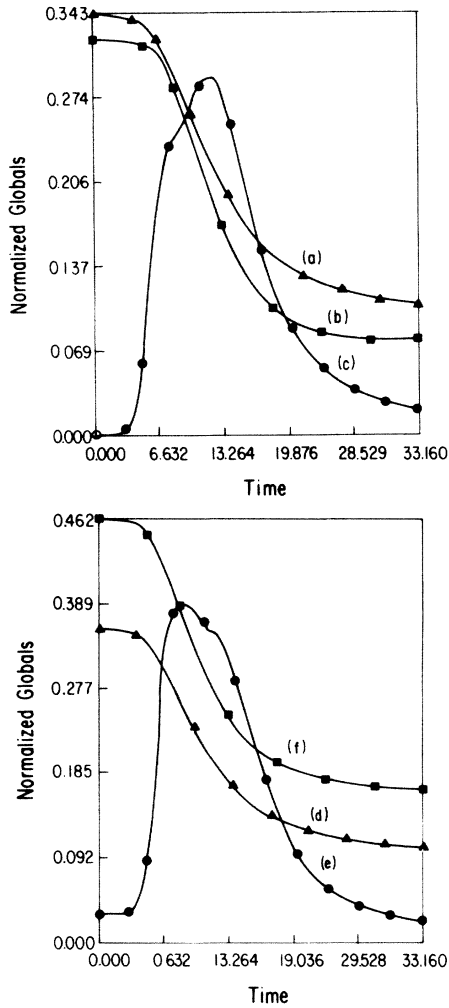


FIG. 2. Decay of global integral quantities, volume averaged: curve *a*, total energy $\times 0.1$; curve *b*, net toroidal current $\times 0.1$; curve *c*, kinetic energy; curve *d*, total magnetic energy $\times 0.1$; curve *e*, total Ohmic dissipation; curve *f*, ratio of total energy to magnetic helicity $\times 0.1$. Time is in units of Alfvén transit time of unit distance.

ventional way. Plotted here, versus k_z , is all the magnetic energy summed up to and including k_z , in a spectral decomposition, and all the Ohmic dissipation, summed up to and including k_z , for the $S = 500$ and $S = 1500$ runs. If the quantity plotted had been fully resolved, perfectly flat spectra at the upper values of k_z would result. Figure 5 seems to indicate that the energy-containing scales of the $S = 500$ run are rather well resolved, but that the dissipation scales are not. The $S = 1500$ run is not well resolved by either measure. The two Kolmogoroff dissipation wave numbers are 55.6 and 130.4, respectively, computed as $[\langle j^2 \rangle / 2\eta^2]^{1/4}$, where $\eta = S^{-1}$.

The precipitous drop in both toroidal current and energy in Fig. 2 is consistent with a recent extension of

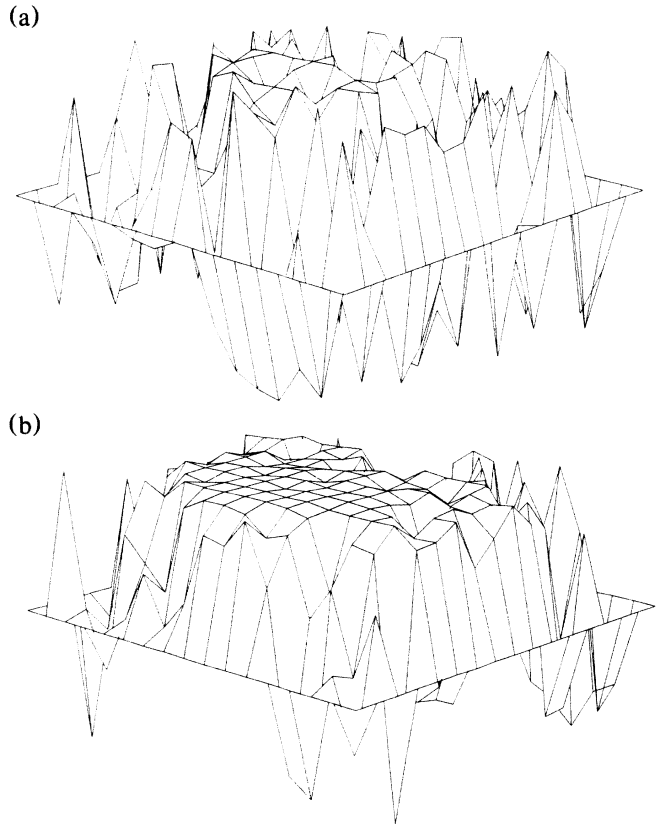


FIG. 3. (a) 3D perspective plot, looking from $x = 0, y = \pi$ in the xy plane, at $z = 0$ and time $t = 19.68$, of the alignment cosine, $\mathbf{j} \cdot \mathbf{B}_{\text{tot}} / jB_{\text{tot}}$, for $S = 500$. (b) Same as (a), but at time $t = 35.04$; relaxation toward a force-free state is apparent.

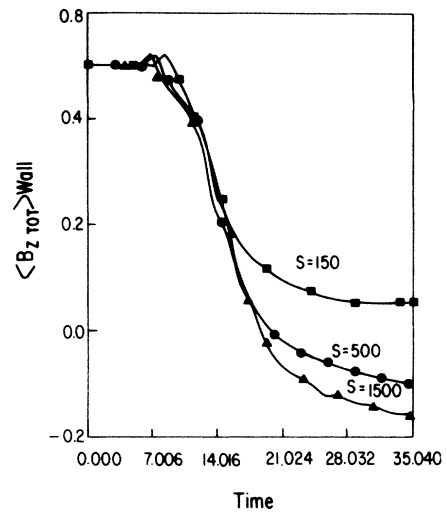


FIG. 4. The average total toroidal magnetic field $\langle B_{\text{tot}z} \rangle$ at the wall, plotted vs time, for $S = 150, 500$, and 1500 runs. The $S = 1500$ run is believed to be poorly resolved, but the field reverses anyway.

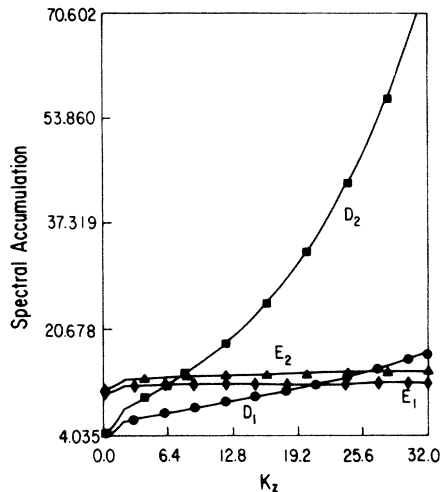


FIG. 5. Four tests of the adequacy of the spatial resolution. Each curve is the total value of a spectrally decomposed positive-definite quantity accumulated between zero and k_z , plotted as a function of k_z . E_1 is $10\times$ magnetic energy for the $S = 500$ run and E_2 is $10\times$ magnetic energy for the $S + 1500$ run. D_1 is the Ohmic dissipation for the $S = 500$ run and D_2 is the Ohmic dissipation for the $S = 1500$ run. A consequence of good resolution for these quantities would be that the curves would be flat to the left of $k_{z\max} = 32$. (The time is 19.68.)

Taylor's theory^{4,6} due to Marklin.²² According to Marklin's (rectangular) calculation, the square-boundary analog of a helical force-free state results when the toroidal current I_z is big enough that the ratio $I_z/B_0\pi^2$ exceeds a minimum which, for our system length 2π , lies at about 1.8. If the relaxation of the toroidal current in Fig. 2 is assumed to be due to the plasma's efforts to get rid of enough energy that this quasihelical state is no longer the minimum-energy one, the ratio $\langle j_z \rangle / B_0 = I_z / B_0\pi^2$ of 1.54 at the end of the run is not far below. The dynamical basis for such a conjecture is not entirely clear, but a likely interpretation is an incompatibility between the helical state and the nonhelical symmetry which the boundary conditions attempt to enforce. This interpretation will be pursued in the future, as will the addition of external electric fields, viscous stresses, and a no-slip boundary condition.

We thank Dr. George Marklin of Los Alamos for informing us of his calculations of rectangular minimum-energy states. Helpful conversations with Dr. R. B. Dahlburg and Dr. J. H. Gardner are appreciated. This work was supported in part by U.S. Department of Energy Grant No. FG02-85ER53194 and NASA Grant No. NAG-W-710 at Dartmouth. The work at

Los Alamos was performed under the auspices of the U.S. Department of Energy.

¹Pulsed High-Beta Plasmas, edited by D. E. Evans (Pergamon, Oxford, 1976).

²J. E. Hammel, D. W. Scudder, and J. S. Schlachter, Nucl. Instrum. Methods **207**, 161 (1983).

³J. D. Sethian, K. A. Gerber, A. G. Robson, A. W. DeSilva, J. E. Hammel, D. W. Scudder, and J. S. Schlachter, in *Proceedings of the Tenth International Conference on Plasma Physics and Controlled Nuclear Fusion Research, London, 1984* (International Atomic Energy Agency, Vienna, 1985).

⁴J. B. Taylor, Phys. Rev. Lett. **33**, 1139 (1974).

⁵J. B. Taylor, in *Proceedings of the Fifth International Conference on Plasma Physics and Controlled Nuclear Fusion Research, Tokyo, Japan, 1974* (International Atomic Energy Agency, Vienna, 1975), Vol. 1, p. 161.

⁶J. B. Taylor, in Ref. 1, pp. 59-67.

⁷D. Montgomery, L. Turner, and G. Vahala, Phys. Fluids **21**, 757 (1978).

⁸W. H. Matthaeus and D. Montgomery, in *Proceedings of the International Conference on Nonlinear Dynamics*, Ann. N.Y. Acad. Sci. **357**, 203 (1980).

⁹W. H. Matthaeus and D. Montgomery, in *Statistical Physics in Chaos and Fusion Plasmas*, edited by C. W. Horton, Jr., and L. E. Reichl (Wiley, New York, 1984), pp. 285-291; W. H. Matthaeus, M. L. Goldstein, and D. Montgomery, Phys. Rev. Lett. **51**, 1484 (1983).

¹⁰S. Riyopoulos, A. Bondeson, and D. Montgomery, Phys. Fluids **25**, 107 (1982).

¹¹A. Sykes and J. A. Wesson, in *Proceedings of the Eighth European Conference on Controlled Fusion and Plasma Physics, Prague, 1977* (Czechoslovak Academy of Sciences, Prague, 1977), p. 80.

¹²R. Horiuchi and T. Sato, Phys. Rev. Lett. **55**, 211 (1985).

¹³A. Hasegawa, Adv. Phys. **34**, 1 (1985).

¹⁴L. Woltjer, Astrophys. J. **130**, 400, 405 (1959), and Proc. Natl. Acad. Sci. U.S.A. **44**, 489 (1958), and **45**, 769 (1959), and Rev. Mod. Phys. **32**, 914 (1960).

¹⁵A. Y. Aydemir and D. C. Barnes, J. Comput. Phys. **53**, 100 (1983), and Phys. Rev. Lett. **52**, 930 (1984); A. Y. Aydemir, D. C. Barnes, E. J. Caramana, A. A. Mirin, R. A. Nebel, D. D. Schnack, and A. G. Sgro, Phys. Fluids **28**, 898 (1985).

¹⁶D. D. Schnack, E. J. Caramana, and R. A. Nebel, Phys. Fluids **28**, 321 (1985).

¹⁷K. A. Werley, R. A. Nebel, and G. A. Wurden, Phys. Fluids **28**, 1450 (1985).

¹⁸In particular, the decaying ratio of energy to helicity was observed in Ref. 12.

¹⁹J. P. Dahlburg, D. Montgomery, and W. H. Matthaeus, J. Plasma Phys. **34**, 1 (1985).

²⁰J. P. Dahlburg, D. Montgomery, G. D. Doolen, and W. H. Matthaeus, J. Plasma Phys. **35**, 1 (1986).

²¹L. Turner and J. Christiansen, Phys. Fluids **24**, 893 (1981); L. Turner, Ann. Phys. (N.Y.) **149**, 58 (1983).

²²G. Marklin, private communication.